Solubility of Lead(II) Oxide and Copper(II) Oxide in Subcritical and Supercritical Water

Kiwamu Sue, Yukiya Hakuta, Richard L. Smith, Jr., Tadafumi Adschiri, and Kunio Arai*

Tohoku University, Department of Chemical Engineering, Aoba-ku, Aramaki-Aza, Aoba-07, Sendai 980-8579, Japan

The solubilities of lead oxide (PbO) and copper oxide (CuO) in subcritical and supercritical water were measured at temperatures from 250 °C to 500 °C and pressures from 26 MPa to 34 MPa, in a flow-type apparatus. The solubility of lead oxide varied from 351 μmol/kg H_2O at 424.9 °C and 25.9 MPa to 4406 μmol/kg H_2O at 350.3 °C and 30.2 MPa. The solubility of copper oxide varied from 1.3 μmol/kg H_2O at 449.8 °C and 28.0 MPa to 8.0 μmol/kg H_2O at 324.9 °C and 28.1 MPa. A hydration reaction model was applied to correlate the data.

Introduction

At elevated temperature, water and metal nitrates react via hydration and dehydration steps to form metal oxides, which subsequently precipitate from solution (Adschiri et al., 1992). This principle has been used to produce new functional materials (Hakuta et al., 1999) and, further, to separate metals from high-level liquid wastewater (Smith et al., 1997). For these applications, phase separation occurs at elevated temperatures and pressures and the solubility of metal oxides at these conditions is essential. Few data exist in the supercritical region, however, due to the difficulty of experimental techniques. In this work, we describe an experimental system that is suitable for measuring metal oxide solubilities in water at supercritical conditions. We report on copper(II) oxide and lead(II) oxide solubilities in subcritical and supercritical water.

Previous literature exists on both of these systems. CuO + water systems have a long history due to their importance in the corrosion mechanism in steam generator power cycles (Palmer et al., 1996). Popcock and Stewart (1963) provided an early set of measurements at 620 °C to 628 °C at pressures from 23 MPa to 31 MPa. Hearn et al. (1969) measured CuO solubilities in water at conditions from 57 °C to 551 °C and at pressures from 7.6 MPa to 41.9 MPa. The two sets of data differ by an order of magnitude. Hearn et al. (1969) attributed these differences to (i) insufficient equilibration times and (ii) use of stainless steel, which would serve as a copper sink. The report of Palmer et al. (1996) notes that the differences between these two detailed studies remain unresolved. In this work, for CuO solubilities in the critical region of water, we show agreement with the data of Hearn et al. (1969).

Materials and Methods

Distilled water used for liquid chromatography analysis and nitric acid solution (1 M) were purchased from Wako Pure Chem. Ltd. (Osaka, Japan). Lead(II) oxide (litharge) and copper(II) oxide were supplied by High Purity Chemical Laboratory (Saitama, Japan) and had purities of 99.99 wt %. Both lead oxide and copper oxide were used in the form of grains (2.0−5.0 mm diameter), which had been formed from research grade sintered powder. The lead oxide and copper oxide had a solid density of 8.7 g/cm^3 and 6.4 g/cm^3, respectively.

Apparatus Development. The challenge in solubility studies is to achieve an equilibrium separation between the solvent (supercritical water) and solute (metal oxide). For near-critical and supercritical water (SCW)−metal oxide systems, this is especially difficult, since the dissolved oxide may recrystallize upon cooling. A method commonly used for electrolyte solubility determination in supercritical water is a semibatch-type method of passing SCW through a salt bed extraction vessel at a low flow rate, which allows the SCW to become saturated at the equilibrium concentration (Armellini and Tester, 1993). Upon exiting the salt bed, the SCW solution is cooled in a cool heat exchanger and brought to atmospheric pressure. The resultant salt-water solution is subsequently sampled and analyzed. This method works very well for salts, such as sodium chloride and sodium sulfate. An assumption in this method is that the salts exhibit a lower solubility at the temperature in the salt bed than that at the temperature within the cool down heat exchanger. However, for the case of measuring metal oxide solubility, if the same approach is applied, the metal oxide would have a tendency to recrystallize within the cool down heat exchanger, since it becomes less soluble at lower temperatures. Ziemniak et al. (1998) measured solubilities of some metal oxides in alkaline media using a similar apparatus to that of Armellini and Tester (1993). In their measurements, plugging or precipitation of the oxide was not a problem due to the low solubilities, use of alkaline media, or restriction of the experiments to subcritical (liquid) conditions. The typical result is plugging of the lines and termination of the experiment under near critical and supercritical conditions. Therefore, we developed a new approach, as described next.

Nitric Acid Mixing Tee. One method to ensure that metals do not precipitated in the cool down portion of the experiment is to mix the metal oxide solution with acid at the given conditions following the extraction. For our experiments, we choose nitric acid, since high-temperature data were available (Oscarson et al., 1992). Nitric acid remains stable, as shown by its ionization constant that can be described by a simple 1/T dependence. Further,

* Corresponding Author. Phone/Fax: +81-22-217-7246.

10.1021/je9901029 CCC: $18.00
Published on Web 11/11/1999

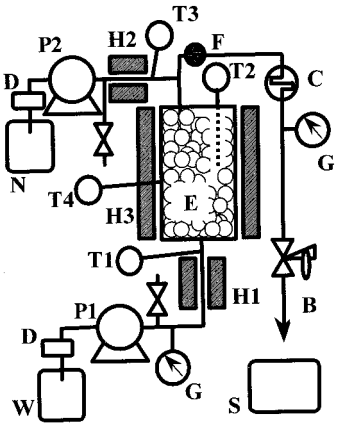

Figure 1. Schematic diagram of experimental apparatus: B, back-pressure regulator; C, cooler; D, degasser; E, equilibrium cell; F, filter; G, gauge (pressure); H, heater; N, nitric acid aqueous solution (1 M); P, pump; S, sample; T, thermocouple; W, water.

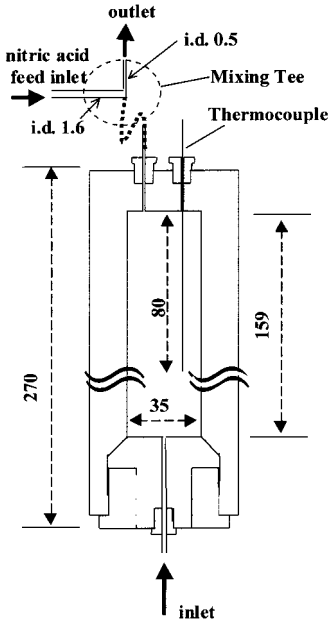

Figure 2. Details of the equilibrium cell; dimensions in millimeters.

nitric acid readily dissolves many metals and oxides. Therefore, suitable introduction of nitric acid can provide a reliable method for ensuring that metal oxides remain in solution.

In the flow method described next, a nitric acid mixing tee was added following the metal oxide saturation step. This allowed for reliable metal oxide solubilities to be determined.

Flow Apparatus. A schematic flow diagram of the experimental apparatus is shown in Figure 1. It consisted of two feed systems, a pressure sensor with an accuracy of ±0.075 MPa, a temperature measurement and control system with an accuracy of 0.1 K, an effluent collection, and an equilibrium cell. The design of the equilibrium cell is shown in Figure 2. It was made of titanium alloy (Ti 6Al 4V) and with dimensions 35 mm i.d., 60 mm o.d., and 159 mm length. The equilibrium cell (manufactured by High Pressure Equipment) was set up horizontally in an electric furnace (Seiwa Riko Corporation., model FTO-6). The oxide crystals were sieved to give a size range of 2.0 to 5.0 mm and were packed loosely (about 560 g) in the equilibrium cell.

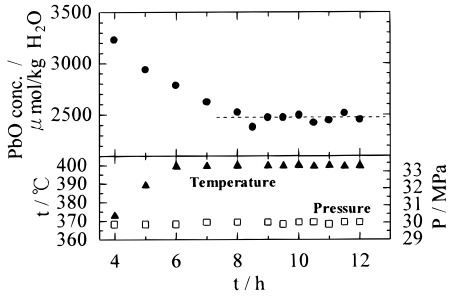

Figure 3. PbO concentration in effluent as a function of time. Conditions: 400.3 °C and 30.0 MPa. Water flow rate: 0.21 g/min.

Distilled water was fed at a rate of 0.19−1.12 g/min by a high-performance liquid chromatography (HPLC) pump 1 (TOA Electronics Corporation, model ICA-3010), whose feed rate was measured by monitoring the weight change of a feed tank with an electric balance (Mettler Toledo Ltd, model PG5002). From another line, 1 M nitric acid solution was fed at a feed rate of 0.21−1.13 g/min by an HPLC pump 2 (TOA Electronics Corporation, model ICA-3011), whose feed rate was measured also by monitoring the weight change of a feed tank with an electric balance (A&D Company, Model FA2000). As shown in Figure 2, the nitric acid mixing tee is connected to the equilibrium cell via an S-shaped trap which reduces the possibility of back flow. A relief valve was installed at the exit of the pump to protect the system from overpressurization.

Both water and nitric acid feed solutions were heated to the extraction temperature (250−500 °C) in SUS 316 tubes (1 m × 0.51 mm i.d., 3.18 mm o.d.) with a H1, H2 electric furnace (Ishizuka Denki Seisakusyo, model 37755). At the end of the cell, an inline filter, F, housing a 0.5 μm sintered stainless steel element (Swagelok, SS-4FWS), was set to retain larger oxide particles during cooling at C. A back pressure regulator, G, (Tescom Corporation, model 26-1700) was used to control system pressure (26−34 MPa) within the accuracy 0.2 MPa.

A three-zone temperature control was employed to ensure that the water temperature at the inlet (T1 in Figure 1), the inside (T2 in Figure 1), and the outside (T4 in Figure 1) of the equilibrium cell and the nitric acid solution temperature at the outlet (T3 in Figure 1) were kept constant. The temperature difference between these three zones was kept to within ±1.0 °C by the electric furnace (H1, H2, and H3, respectively) by using a PID controller with a chromel−alumel thermocouple. Measurements of pressure, temperature, and flow rate were recorded at 5−15 min intervals. A typical run is shown in Figure 3.

The cell effluent solution was collected every 15 min for 10−12 h in a glass flask and weighed with an analytical balance (Mettler Toledo Ltd, model AE200). Metal (Pb, Cu, Fe, Cr, Mo, Ni, Ti) ion concentrations were measured with an inductively coupled plasma spectrometer (ICP) (Seiko, model SPS-1200). A typical detection limit was 0.1 ppm (w/w) metal. Nitrate and nitrite concentrations were measured with ion chromatography (IC) with a column (TOA Electronics Corporation, model PCI-201S) and with phthalic acid/hydroxymethyl aminomethane solution as the mobile phase. The filter and S-shaped trap were checked at the end of each experimental run. No solid materials were found.

With known concentrations, the mass flow rates of all species in the feed and effluent, and mass and ion balances were calculated, and the lead (or copper) ion concentration saturated in the equilibrium cell was determined. The

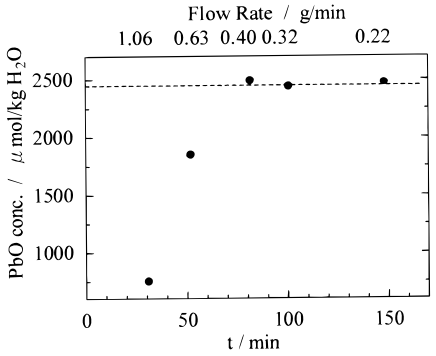

Figure 4. PbO concentration in effluent as a function of residence time. Conditions: 400 °C and 30 MPa.

Table 1. Solubility of Copper Oxide in Subcritical and Supercritical Water

t/°C	*P*/MPa	*S*/μmol/kg H_2O
299.8 ± 0.1	28.1 ± 0.1	7.8 ± 0.3
324.9 ± 0.2	28.1 ± 0.2	8.0 ± 0.3
350.0 ± 0.1	28.0 ± 0.1	6.7 ± 0.3
375.3 ± 0.3	28.2 ± 0.1	4.5 ± 0.2
400.1 ± 0.2	27.9 ± 0.1	2.5 ± 0.1
425.2 ± 0.1	28.0 ± 0.1	1.3 ± 0.1
449.8 ± 0.2	28.0 ± 0.2	1.3 ± 0.1

concentration of lead (or copper) ion was determined as an average of the value of the plateau values (Figure 3). The experimental error of the measured solubility is reported as the standard deviation of the concentration data.

Results and Discussion

Solubility. The flow method used depends on the solution becoming saturated with metal oxide during the solvent's residence time in the equilibrium cell. To ascertain that the effluent solution was saturated, we measured the variation of the effluent ion concentration with residence time. Figure 4 shows the relationship between the lead oxide concentration and the residence time for a lead oxide−water system at 400 °C and 30 MPa. The residence time was calculated by the following equations:

$$\tau = \frac{V - V_{PbO}}{F/\rho} \qquad (1)$$

where V is the cell volume, V_{PbO} is the volume of lead oxide based on the density and weight, F is the flow rate of water at room temperature, and ρ is the water density, 0.358 g/cm^3, at 400 °C and 30 MPa.

As shown in Figure 4, it was found that the effluent solution required a residence time of at least 1.5 h to become saturated with lead oxide, which corresponds to flow rates < 0.35 g/min. Therefore, we set the flow rate < 0.30 g/min in all the following runs. The residence times were between 1.5 h and 2.5 h for each set of experimental data at a given temperature and pressure.

The experimental results of the copper oxide solubility are shown in Table 1. The estimated errors in Table 1 were determined by the 95% confidence interval of steady-state runs at 400.1 °C and 27.9 MPa. The present results are compared with the literature data (Hearn et al., 1969) in Figure 5. The present results show good agreement with the literature data.

The experimental lead oxide solubilities determined are shown in Table 2 and are plotted versus temperature in Figure 6. The estimated errors in Table 2 were determined by the 95% confidence interval of steady-state runs at 400.3 °C and 30.0 MPa. Also shown are the data of Yokoyama et al. (1993), who measured lead oxide solubilities with a one-path flow apparatus at several temperatures. The data have a similar trend to that of Yokoyama et al. (1993) with solubility increasing as pressure increases and a dramatic decrease in solubility as temperature increases into the supercritical region.

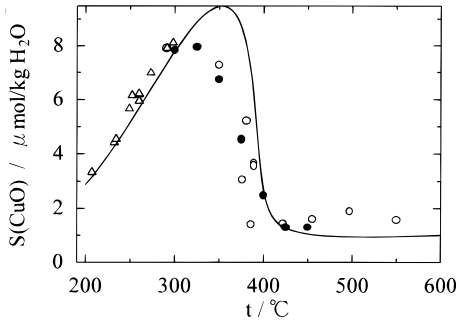

Figure 5. Predicted and measured CuO isobaric solubility behavior in subcritical and supercritical water. Symbols definitions: ●, this work (28 MPa); ○, Hearn et al. (28 MPa); △, Hearn et al. (saturation); line, eq 11.

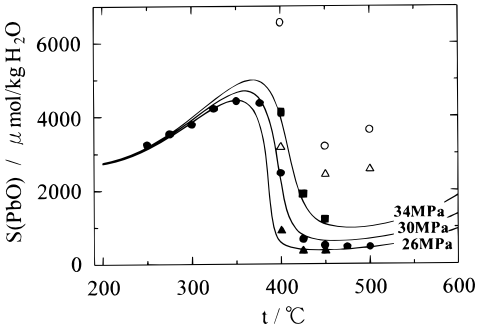

Figure 6. Predicted and measured PbO isobaric solubility behavior in subcritical and supercritical water. Symbols definitions: ■, this work (34 MPa); ●, this work (30 MPa); ▲, this work (26 MPa); ○, Yokoyama et al. (30 MPa); △, Yokoyama et al. (26 MPa); lines, eq 10.

Table 2. Solubility of Lead Oxide in Subcritical and Supercritical Water

t/°C	*P*/MPa	*S*/μmol/kg H_2O
250.0 ± 0.2	30.0 ± 0.2	8246 ± 45
275.6 ± 0.3	30.3 ± 0.3	3531 ± 49
300.5 ± 0.3	29.9 ± 0.2	3778 ± 53
325.3 ± 0.3	30.2 ± 0.4	4205 ± 59
350.3 ± 0.3	30.2 ± 0.4	4406 ± 62
376.5 ± 0.3	30.3 ± 0.3	4358 ± 61
400.3 ± 0.1	30.0 ± 0.1	2466 ± 34
425.3 ± 0.0	30.0 ± 0.1	673 ± 9
449.5 ± 0.2	29.9 ± 0.1	502 ± 7
475.3 ± 0.2	30.1 ± 0.1	459 ± 6
500.8 ± 0.1	30.0 ± 0.1	468 ± 7
400.5 ± 0.3	26.0 ± 0.2	900 ± 13
424.9 ± 0.3	25.9 ± 0.2	351 ± 5
450.0 ± 0.2	26.3 ± 0.2	353 ± 5
400.7 ± 0.2	34.0 ± 0.2	4107 ± 57
425.1 ± 0.2	34.1 ± 0.2	1897 ± 27
450.1 ± 0.2	34.3 ± 0.1	1201 ± 17

Corrosion Tests. Corrosion of the reactor was examined to detect possible leaching of metals from the titanium equilibrium cell, the stainless tubing, or other sources. These have been reported as possible sinks for the copper ions that might produce systematic error (Palmer et al., 1996). First, water was heated to supercritical conditions and fed (0.21 g/min) into an empty equilibrium cell. The nitric acid mixing tee was not used for this case. No metals

could be detected in the effluent within the limits of the ICP.

Then, aqueous nitric acid fed (0.23 g/min) into the mixing tee. For this case, the detected metal concentrations in the effluent were Fe (12.7 mg/kg), Ni (4.1 mg/kg), and Mo (1.9 mg/kg). Chromium and titanium could not be detected. The nitrate and nitrite concentrations in the effluent were measured with ion chromatography. The nitrate concentration agreed with the material balance. No nitrites were detected. Moreover, no gas was observed in any of the runs.

Data Correlation. In this study, we applied the hydration reaction model (Wendlandt and Glemser, 1964) for the solvation of lead oxide (or copper oxide) in high-temperature water. According to this model, general reactions between lead oxide (or copper oxide) and high-temperature water, and the equilibrium constant K are expressed as follows:

$$\mathrm{PbO(solid)} + n\mathrm{H_2O} \leftrightarrow \mathrm{PbO}\cdot n\mathrm{H_2O} \tag{2}$$

$$K_1 = \frac{[\mathrm{PbO}\cdot n\mathrm{H_2O}]}{[\mathrm{H_2O}]^n} \tag{3}$$

$$\mathrm{CuO(solid)} + n\mathrm{H_2O} \leftrightarrow \mathrm{CuO}\cdot n\mathrm{H_2O} \tag{4}$$

$$K_2 = \frac{[\mathrm{CuO}\cdot n\mathrm{H_2O}]}{[\mathrm{H_2O}]^n} \tag{5}$$

where n is the hydration number. Equation 2−5 are based on the assumption that the concentrations of the lead (or copper) ion and the ion hydrocomplexes are small due to the low dielectric constant of high-temperature water. Furthermore, in dilute solutions, the concentrations do not differ appreciably from the thermodynamic activities. In the usual manner, the thermodynamic activity of a pure solid-phase reference state is taken to be unity.

For these reactions, the equilibrium constant can be changed as follows:

$$\ln K_1 = \ln[\mathrm{PbO}\cdot n\mathrm{H_2O}] - n \ln [\mathrm{H_2O}]$$

$$= \ln[\mathrm{PbO}\cdot n\mathrm{H_2O}] - n \ln 55.51 - n \ln \rho \tag{6}$$

$$\ln K_2 = \ln[\mathrm{CuO}\cdot n\mathrm{H_2O}] - n \ln [\mathrm{H_2O}]$$

$$= \ln[\mathrm{CuO}\cdot n\mathrm{H_2O}] - n \ln 55.51 - n \ln \rho \tag{7}$$

where concentrations are given in moles per kilogram of H_2O, 55.51 is moles of H_2O per kilogram of H_2O, and ρ is the pure water density (g/cm^3) at the given conditions. The density of the water was obtained from Haar et al. (1984).

The equilibrium constant K at temperature T is estimated by the thermodynamic relationships

$$\Delta G = -RT \ln K \tag{8}$$

and

$$\Delta G(T) = \Delta H(T) - T\Delta S(T)$$

$$= \Delta H(298) - T\Delta S(298) + \int \Delta C_\mathrm{p}\, \mathrm{d}T - T\int (\Delta C_\mathrm{p}/T)\, \mathrm{d}T$$

$$= A - BT - CT \ln T \tag{9}$$

where

Table 3. Density Model (Eqs 10 and 11) Parameters

	A'	B'	C'	D'
CuO	8.6	3430	0.5	1.90
PbO	162	−9500	22.0	2.15

$$A = \Delta H(298) - 298\Delta C_\mathrm{p}$$

$$B = \Delta S(298) - (1 + \ln 298)\Delta C_\mathrm{p}$$

$$C = \Delta C_\mathrm{p}$$

In this analysis, ΔC_p was assumed to be constant. From eqs 6−9, the solubilities (equilibrium constants) in subcritical and supercritical water were correlated as a function of density and temperature using the following semiempirical form (Marshall, 1970; Ziemniak, 1992):

$$\ln [\mathrm{PbO}\cdot n\mathrm{H_2O}] = A' - \frac{B'}{T} + C' \ln T + D' \ln \rho \tag{10}$$

$$\ln [\mathrm{CuO}\cdot n\mathrm{H_2O}] = A' - \frac{B'}{T} + C' \ln T + D' \ln \rho \tag{11}$$

where the coefficients A', B', C', and D' are fitting parameters and ρ is the water density (g/cm^3). The density of the water was obtained from Haar et al. (1984).

The parameters A', B' , C', and D' were determined by Marquardt's method of fitting the solubility data with the following objective function:

$$\min \frac{1}{N}\sum_{i=1}^{N} (\ln S_i^{\mathrm{cal}} - \ln S_i^{\mathrm{exp}}) \tag{12}$$

where N is the number of data points and S_i^{cal} and S_i^{exp} are the calculated and experimental solubility, respectively.

Table 3 shows the parameters determined through the fitting with this model.

The parameter uncertainties were estimated from the covariance matrix. For CuO, they were 1.1, 70, 0.15, and 0.01 for A', B' , C', and D', respectively. For PbO, they were 8.6, 690, 1.2, and 0.01 for A', B' , C', and D', respectively. The constants given in Table 3 give an error in solubility of $\pm 9.8 \times 10^{-7}$ mol CuO/kg H_2O and $\pm 2.5 \times 10^{-4}$ mol PbO/kg H_2O over the full range of conditions studied except in the vicinity of the critical point. This is probably due to the treatment of D', which is related to the mean hydration number, in eqs 10 and 11, as a constant. As shown in Figures 5 and 6, the copper oxide and lead oxide solubility curves can be correlated by use of the hydration reaction model.

Conclusions

A flow apparatus was developed for determining the solubilities of metal oxides in SCW. Following SCW−oxide saturation, aqueous nitric acid is mixed with the solution to prevent precipitation and allow simplified composition analysis. Measurements made of the CuO system agreed with the data of Hearn et al. (1969). New data are reported for PbO. A semiempirical density model could correlate the data as a function of water density and temperature.

Literature Cited

Adschiri, T.; Kanazawa, K.; Arai, K. Rapid and Continuous Hydrothermal Crystallization of Metal Oxide Particles in Supercritical Water. *J. Am. Ceram. Soc.* **1992**, *75* (4), 1019−1022.

Armellini, F.; Tester, J. Solubilities of Sodium Chloride and Sodium Sulfate in Sub and Supercritical Water from 450 to 550 °C and 100−250 bar. *Fluid Phase Equilib.* **1993**, *84*, 123−142.

Hakuta, Y.; Adschiri, T.; Hirakoso, H.; Arai, K. Chemical Equilibria and Particle Morphology of Boehmite (AlOOH) in Sub and Supercritical Water. *Fluid Phase Equilib.* **1999**, *158*, 733−742.

Hearn, B.; Hunt, M.; Hayward, A. Solubility of Cupric Oxide in Pure Subcritical and Supercritical Water. *J. Chem. Eng. Data* **1969**, *14*, 442−447.

Marshall, W. Complete Equilibrium Constants, Electrolyte Equilibria, and Reaction Rates. *J. Phys. Chem.* **1970**, *74*, 346−355.

Oscarson, J. L.; Gillespie, S. E.; Izatt, R. M.; Chen, X.; Pando, C. Thermodynamic Quantities for The Ionization of Nitric Acid in Aqueous Solution from 250 to 319 °C. *J. Solution Chem.* **1992,** *21* (8), 789−801.

Palmer, D. A.; Simonson, J. M.; Joyce, D. B. Volatility of Copper. Electric Power Research Institute Sponsored Conference (CONF-9606259- -1) 1996, Periche, Italy.

Popcock, E. J.; Stewart, J. F. The Solubility of Copper and It's Oxide in Supercritical Steam. *J. Eng. Power* **1963**, 33−45.

Smith, R.; Atmaji, P.; Hakuta, Y.; Kawaguchi, M.; Adschiri, T.; Arai, K. Recovery of Metals from Simulated High-Level Liquid Waste with Hydrothermal Crystallization. *J. Supercrit. Fluids* **1997**, *11*, 103−114.

Wendlandt, H.; Glemser, O. The Reaction of Oxides with Water at High Pressure and Temperatures. *Angew. Chem., Int. Ed. Engl.* **1964**, *3*, 47−54.

Yokoyama, C.; Iwabuchi, A.; Takahashi, S. Solubility of PbO in Supercritical Water. *Fluid Phase Equilib.* **1993**, *82*, 323−331.

Ziemniak, S. Metal Oxide Solubility Behavior in High-Temperature Aqueous Solutions. *J. Solution Chem.* **1992**, *21* (8), 745−760.

Ziemniak, S.; Jones, M.; Combs, K. Solubility and Phase Behavior of Cr(III) Oxides in Alkaline Media at Elevated Temperatures. *J. Solution Chem.* **1998**, *27* (1), 33−66.

Received for review April 12, 1999. Accepted September 14, 1999.

JE9901029